

Efficient Visible-Light Photocatalytic Degradation of Rhodamine-B Dye based on Water-Stable (4,4'-VDP)Pb₂Br₆ Perovskites

Jie Feng¹, Junlin Wang¹, Fan Wu³, Chao Wang^{1, 2, 3, 4, 5*}

1. National-Provincial Joint Engineering Research Center of Biomaterials for Machinery Package, Institute of Opto-Mechanical and Electrical Instrument Engineering, Nanjing Forestry University, Nanjing 210037, China

2. Zhejiang Province Key Laboratory of Quantum Technology and Device, Zhejiang University, Hangzhou 310027, China

3. Huzhou Key Laboratory of Materials for Energy Conversion and Storage, Huzhou University, Huzhou 313001, P. R. China

4. National Laboratory of Solid State Microstructures, Nanjing University, Nanjing 210093, China.

5. Key Laboratory of Computational Physical Sciences (Fudan University), Ministry of Education, Shanghai 200438, China.

Corresponding Author: wangchao@njfu.edu.cn;

1. Experimental section

1.1 Chemicals: 1,2-bis (4-pyridinyl) ethylene (4,4'-VDP: $C_{12}H_{10}N_2$), lead bromide (Br_2Pb), hydrogen bromide (HBr) and hypophosphous acid (H_3PO_2) were purchased from Aladdin (Shanghai, China).

1.2 Synthesis of (4,4'-VDP) Pb_2Br_6 : Add 0.5 mmol (183.5 mg) and 0.5mmol (91 mg) of 4,4'-VDP to a three-mouthed flask and dissolve them in 50 mL of HBr and 3 mL of H_3PO_2 . Under constant magnetic stirring, heat to 120 °C.

1.3 Characterization: Powder X-ray diffraction (XRD) was conducted on a Bruker D8 ADVANCE X-ray diffractometer equipped with a Cu $K\alpha$ X-ray tube ($\lambda = 1.54186 \text{ \AA}$). Energy dispersive X-ray spectroscopy (EDS) was performed using a field emission scanning electron microscope (JSM-7600F). Scanning electron microscope (SEM) images were captured by a Nova Nano SEM 450. Decay profiles were collected using a transient steady-state fluorescence spectrometer (FluoroMax-4). X-ray photoelectron spectroscopy (XPS) tests were performed using an X-ray photoelectron spectrometer (AXIS UltraDLD). The PL/PLE spectra and pseudo-color map was measured by a fluorescence spectrophotometer (FL970). The absorbance graph was collected by an ocean optics.

1.4 Electrochemical testing: The transient photocurrent, electrochemical impedance and Mott-Schottky plot of the samples were collected using an electrochemical workstation. A three-electrode system is adopted (Counter electrode: Platinum sheet, Reference electrode: Ag/AgCl, Working electrode: 7 mg (4,4'-VDP) Pb_2Br_6 was dropped onto the FTO). The electrolyte was an acetonitrile solution containing 0.1 M tetrabutylammonium hexafluorophosphate.

1.5 DFT calculation: Periodic density functional theory (DFT) calculations were performed using the Vienna Ab initio Simulation Package (VASP). Generalized Gradient Approximation (GGA), Perdew-Burke-Ernzerhof (PBE) functional and Heyd-Scuseria Ernzerhof 2006 (HSE06) were adopted. The Projected Enhanced Wave (PAW) method is utilized for structural optimization, static self-consistent field calculation, Density of States (DOS) analysis and energy band calculation. A

Brillouin zone integral is carried out using a 311 Monkhorst-Pack K-point grid plane-wave cutoff energy of 400 eV was adopted. The electron convergence criterion was set at 1.0×10^{-5} eV/atom, and the force convergence criterion was set at 0.01 eV/Å.

1.6 Photocatalytic experiments: The photocatalytic degradation of RhB aqueous solution was carried out in the presence of (4,4'-VDP)Pb₂Br₆ perovskite materials. The dosage of RhB is 2mg per 30mL of aqueous solution and the loading of the photocatalyst is 20mg in 10mL of RhB solution. Stir for one hour in a dark environment to reach adsorption equilibrium before irradiation. Irradiation was carried out using a xenon lamp ($\lambda > 400\text{nm}$). The RhB solutions obtained under different illumination times were subjected to threefold dilution prior to absorbance measurement.

1.7 Concentration calculation: The same amount of solution was taken at different time points during the irradiation process and the concentration change of the solution was determined by absorption spectroscopy. A series of RhB solutions of known concentrations were prepared. The absorbance graphs of samples of different concentrations were collected using an ocean optics to obtain the function curve of concentration and absorbance, which was used to calculate the solution concentration at different irradiation times.

2. The spectra and data selected in this article



Figure S1. SEM image of (4,4'-VDP)Pb₂Br₆.

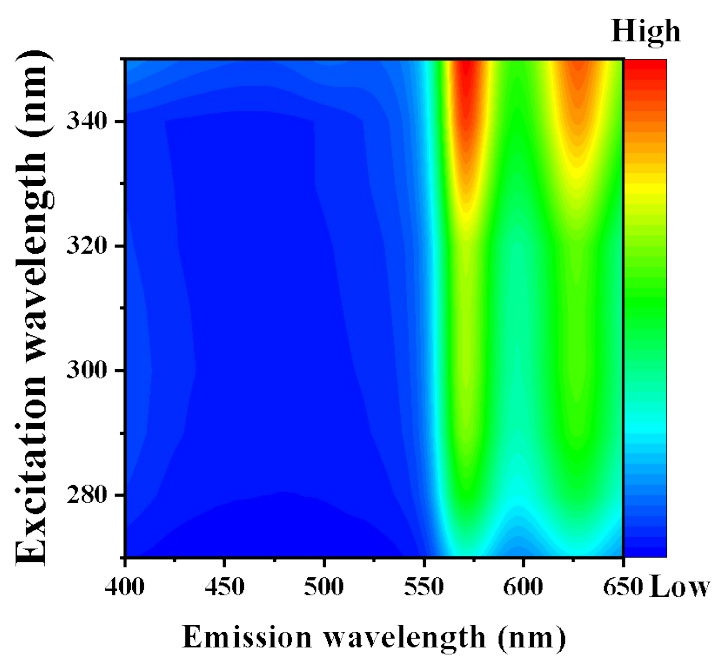


Figure S2. Pseudo-color map of the wavelength-dependent PLE spectrum of (4,4'-VDP)Pb₂Br₆.

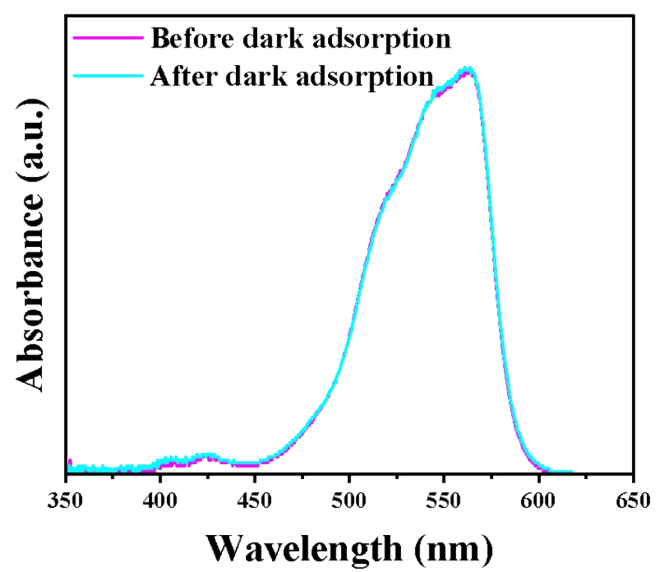


Figure S3. UV/vis spectra of RhB coexisting with (4,4'-VDP) Pb₂Br₆ before and after dark adsorption.

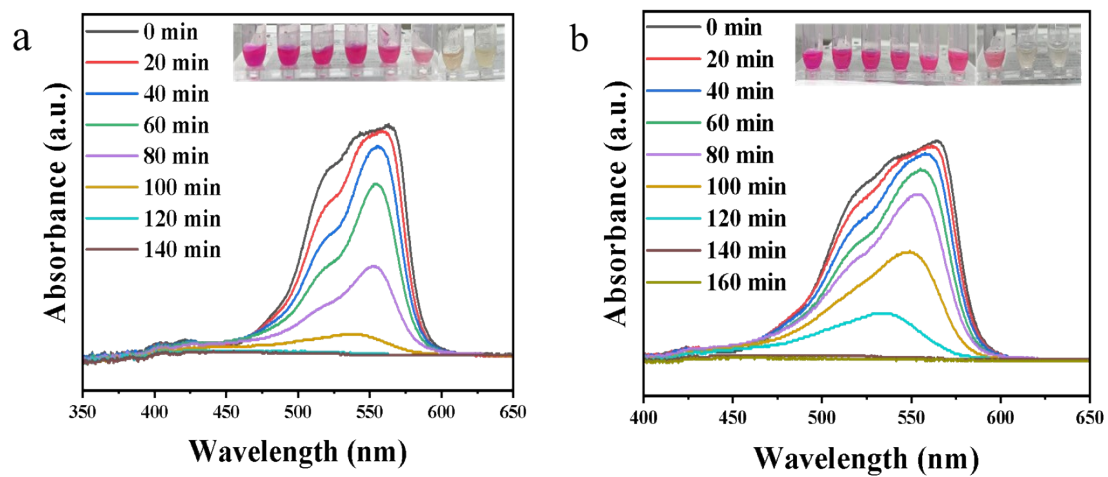


Figure S4. UV/vis spectra of RhB in the presence of (4,4'-VDP)Pb₂Br₆ at different irradiation times (Inset: Digital photos of RhB at different irradiation times): a) 300.15 K. b) 310.15 K.

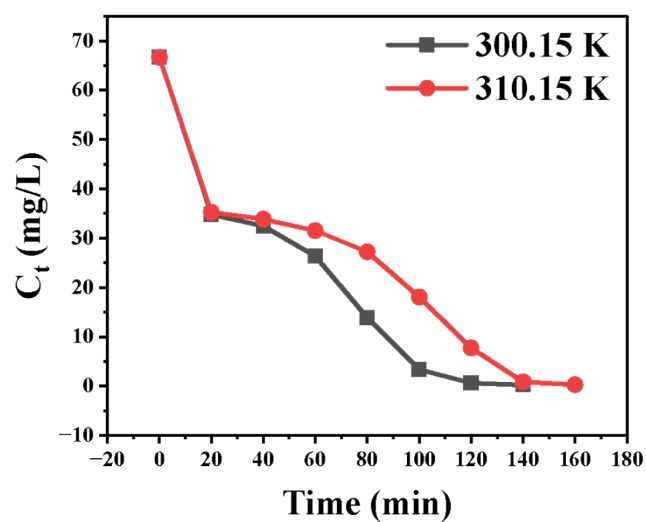


Figure S5. Concentration variation curves of RhB degraded by (4,4'-VDP)Pb₂Br₆ at different temperatures (300.15 K, 310.15 K).

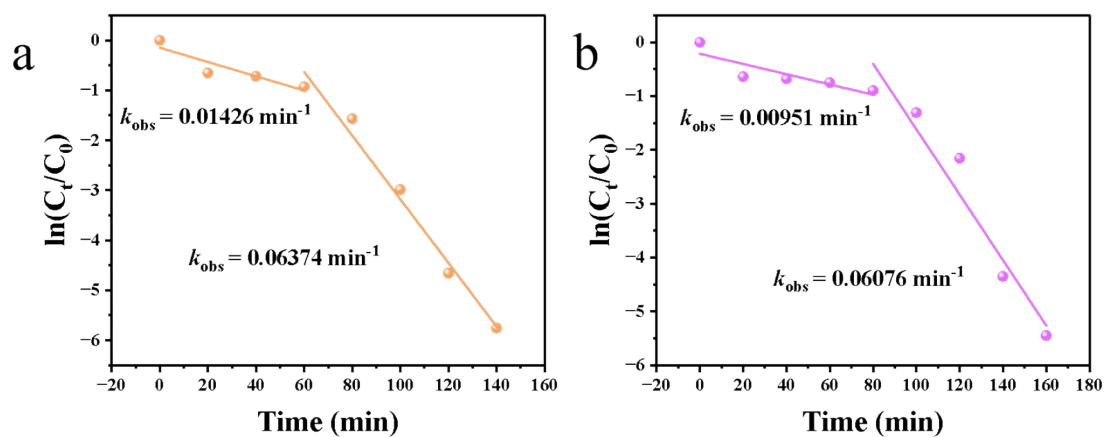


Figure S6. Kinetic curve of RhB dye degradation: a) 300.15 K. b) 310.15 K.

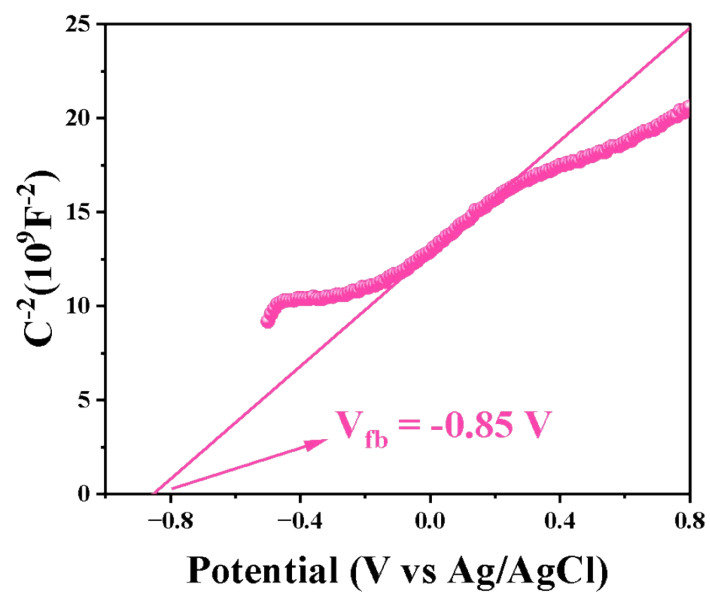


Figure S7. Mott-Schottky plots of (4,4'-VDP) Pb_2Br_6 .

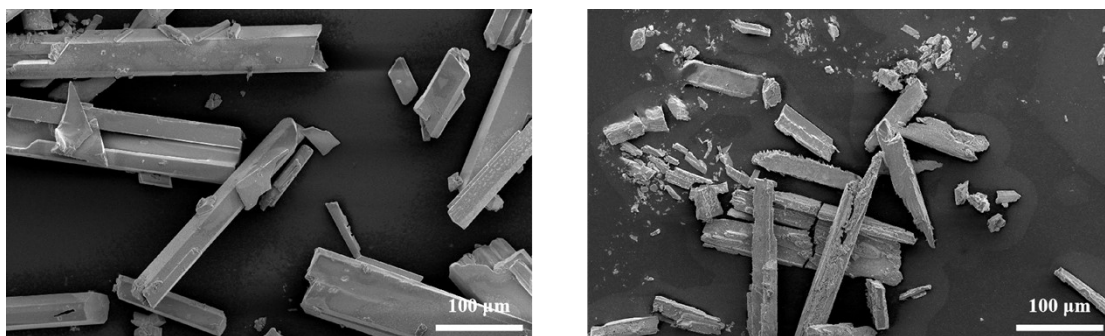


Figure S8. SEM images of (4,4'-VDP) Pb_2Br_6 before (left) and after (right) five photocatalytic cycles.

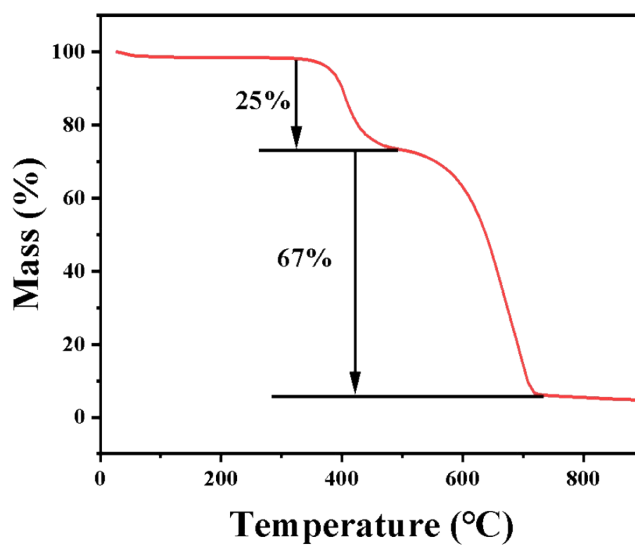


Figure S9. Thermogravimetric (TG) curve of (4,4'-VDP) Pb_2Br_6 .